Journal of Zhejiang University-SCIENCE A (Applied Physics & Engineering)
ISSN 1673-565X (Print); ISSN 1862-1775 (Online)
www.jzus.zju.edu.cn; link.springer.com
E-mail: jzus_a@zju.edu.cn

Dynamic response of bilayered saturated porous media based on fractional thermoelastic theory[#*]

Min-jie WEN[†1,2], Kui-hua WANG[1,2], Wen-bing WU[3], Yun-peng ZHANG[3], Hou-ren XIONG[4]

[1]*Research Center of Coastal Urban Geotechnical Engineering, Zhejiang University, Hangzhou 310058, China*

[2]*MOE Key Laboratory of Soft Soils and Geoenvironmental Engineering, Zhejiang University, Hangzhou 310058, China*

[3]*Engineering Research Centre of Rock-Soil Drilling & Excavation and Protection, Ministry of Education, Faculty of Engineering, China University of Geosciences, Wuhan 430074, China*

[4]*Jiaxing Key Laboratory of Building Energy Efficiency Technology, Jiaxing University, Jiaxing 314001, China*

[†]E-mail: 0620577@zju.edu.cn

Received Feb. 20, 2021; Revision accepted June 25, 2021; Crosschecked Nov. 22, 2021

Abstract: Considering the thermal contact resistance and elastic wave impedance at the interface, in this paper we theoretically investigate the thermo-hydro-mechanical (THM) coupling dynamic response of bilayered saturated porous media. Fractional thermoelastic theory is applied to porous media with imperfect thermal and mechanical contact. The analytical solutions of the dynamic response of the bilayered saturated porous media are obtained in frequency domain. Furthermore, the effects of fractional derivative parameters and thermal contact resistance on the dynamic response of such media are systematically discussed. Results show that the effects of fractional derivative parameters on the dynamic response of bilayered saturated porous media are related to the thermal contact resistance at the interface. With increasing thermal contact resistance, the displacement, pore water pressure, and stress decrease gradually.

Key words: Bilayered saturated porous media; Thermo-hydro-mechanical (THM) coupling dynamic response; Fractional thermoelastic theory; Thermal contact resistance; Elastic wave impedance

https://doi.org/10.1631/jzus.A2100084 **CLC number:** TU473.4

1 Introduction

The thermo-hydro-mechanical (THM) coupling theory of porous media is of great importance in civil and energy engineering (Mei and Yin, 2008, Li CX et al., 2010, 2012, 2017, 2020; Li and Xie, 2013; Mei and Chen, 2013; Zhang et al., 2021). Numerous practical projects, such as extraction of geothermal energy, storage of thermal fluids, and deep geological disposal of radioactive waste, need to carry out THM coupling analysis before construction (Levy et al., 1995; Liu et al., 2010b; Tao et al., 2014). Therefore, considering the neglect of fluid flux in the thermoelasticity, a detailed and in-depth understanding of hydrothermal, hydromechanical, and thermomechanical processes is necessary for describing the coupling behavior of fluid-saturated media (Liu et al., 2009). To overcome the shortcomings of the classical uncoupled and coupled thermoelastic theory which assumes the thermal wave propagates at infinite velocity (Biot, 1956; Booker and Savvidou, 1984; Wang et al., 2013; Zhang et al., 2022), generalized thermoelastic theory and diffusions theory have been proposed (Lord and Shulman, 1967;

[*] Project supported by the National Natural Science Foundation of China (Nos. 52108347 and 51779217), the Primary Research and Development Plan of Zhejiang Province (Nos. 2019C03120 and 2020C01147), China

Electronic supplementary materials: The online version of this article (https://doi.org/10.1631/jzus.A2100084) contains supplementary materials, which are available to authorized users

ORCID: Min-jie WEN, https://orcid.org/0000-0001-7566-7131; Kui-hua WANG, https://orcid.org/0000-0002-9362-0326

Green and Lindsay, 1972; Abbas and Marin, 2018; Abbas et al., 2019).

Many studies based on the above theories have been applied to specific cases. Sherief and Hussein (2012) developed a THM coupling mathematical model with two temperatures for porous media, and analyzed the transient response of semi-infinite thermoelastic media subjected to thermal impact. Liu et al. (2010a) investigated the thermo-viscoelastic dynamic response of saturated porous media. Lu et al. (2010) focused on the dynamic thermo-mechanical response of half-space saturated poroelastic media and summarized the differences in response between thermoelastic and saturated porous thermoelastic media. Xue et al. (2020) studied the coupled thermal-moisture response of a cylinder with circular cracks and determined the effect of relaxation time on the response. Based on the two-temperature theory, Hussein (2018) theoretically investigated the effect of porosity on the temperature increment, displacement, and pore water pressure of solids and fluids. Singh (2013) used the generalized thermoelastic model to analyze the propagation and attenuation characteristics of elastic waves in saturated porous thermoelastic media. Saeed et al. (2020) investigated the dynamic thermoelastic response of saturated porous materials by finite element method. Youssef (2007) adjusted the generalized thermoelastic theory based on the Lord-Shulman (L-S) thermoelastic model. Bhatti et al. (2020) presented a theoretical study on the swimming of migratory gyrotactic microorganisms in a non-Newtonian blood-based nanofluid via an anisotropically narrowing artery. Khan et al. (2019) examined a third-grade magnetohydrodynamic fluid with variable thermal conductivity and chemical reaction over an exponentially stretched surface. Alzahrani and Abbas (2020) used finite element method to investigate the generalized thermoelastic response of saturated porous materials.

Note that all the above-mentioned solutions neglect the different heat conduction phenomena in the process of thermal wave propagation, and the temperature field of saturated porous media cannot be described by the generalized thermoelastic theory at high temperatures. To address this problem, Sherief et al. (2010) and Sherief and El-Latief (2015) derived an equation of generalized thermoelasticity with a fractional derivative, and Youssef (2010) proposed a damped version of Fourier's law using time-fractional derivative theory. Subsequently, some researchers used fractional thermoelastic theory to investigate the dynamic response of saturated porous media or thermoelastic media. Ezzat et al. (2015) introduced a heat conduction model with a fractional derivative to investigate the dynamic response of half-space porous media. Based on fractional thermoelastic theory, Sherief and El-Latief (2013) derived a semi-analytical solution to the temperature-dependent heat conduction coefficient. Deswal and Kalkal (2013) analyzed the thermo-viscoelastic behavior of fractional micropolar media based on the two-temperature theory. Hussein (2015) focused on the fractional thermoelastic problem of an infinite cylinder and investigated the effects of fractional derivative parameters on the response. Sherief and El-Latief (2015) analyzed the fractional thermoelastic problem of thermoelastic media with a spherical cavity. Hobiny and Abbas (2021) established a bio-heat model with a fractional derivative to study the variations of temperature and thermal damage in spherical tissues during thermal therapy. In addition, Hobiny and Abbas (2020) proposed a mathematical model based on Green-Naghdi photothermal theory of fractional-order heat transfer to study wave propagation in a 2D semiconductor material. Considering the temperature-dependent characteristics of materials, Peng et al. (2020) studied the fractional thermal diffusion problem in infinite thermoelastic media with a spherical cavity. Alzahrani et al. (2020) investigated the behavior of a 2D porous material under weak, strong, and normal conductivity using the eigenvalues method. By introducing a time fractional derivative of the Taylor-Riemann series into the heat conduction equation, Wen et al. (2020) investigated the dynamic response of a circular tunnel in saturated porous thermoelastic media.

Differences among thermophysical parameters of each layer have a great influence on the distribution of physical fields in saturated porous media. Ai and Wang (2015a) focused on the axisymmetric thermal consolidation of layered saturated porous media due to a heat source. They investigated the 3D THM coupling response of saturated porous thermoelastic media (Ai and Wang, 2016). Ai et al. (2018) laid emphasis on the axisymmetric thermal consolidation problem of layered transversely isotropic soil

and studied the effects of transversely isotopic parameters on the displacement, temperature, pore water pressure, and stress of soil. Wang and Wang (2020) investigated the long-term thermal consolidation properties of layered saturated soft soil and derived a semi-analytical solution of a saturated soft soil foundation under different rheological models via Laplace and Hankel transform. Considering the thermal diffusion effect, Ai and Wang (2015b) studied the 3D thermo-mechanical coupling response of layered saturated porous media. In the above studies, the interface of layered saturated porous media was simplified as perfect contact, and the effect of thermal contact resistance was ignored.

Due to microscopic unevenness at the interface, the interaction between two interfaces generally occurs at discrete contact points. When heat flux passes through the first layer of media, the area of the contact surface shrinks, resulting in a reduction of heat and the formation of thermal contact resistance (Fig. 1) (Kek-Kiong and Sadhal, 1992). It has been reported that the thermal contact resistance is generated by the coupling effect of three factors, i.e. heat, force, and material, and is also affected by the surface roughness and material properties of the contact media (Yovanovich, 2005). Carr and March (2018) developed four different thermal contact resistance models for layered thermoelastic media. Xue et al. (2016) constructed an incomplete interface contact model and investigated the thermo-mechanical coupling response of a bilayer media based on the generalized fractional thermoelastic model. In another study, Xue et al. (2017) further introduced a heat diffusion effect to analyze the transient response of multi-layer structures in the presence of thermal contact resistance. In a subsequent study, they explored the transient response of layered thermoelastic media with temperature-dependent thermal diffusivity and heat conductivity (Xue et al., 2019). Li CL et al. (2020) employed generalized thermo-viscoelastic fractional strain theory to investigate the thermo-mechanical response of a layered viscoelastic composite structure interface under non-ideal contact. Yuan et al. (2021) correlated the thermo-physical properties of a material with temperature and investigated the nonlocal thermodynamic response of an external thermal insulation system. He et al. (2019) analyzed the transient response of a spherical shell embedded in an infinite thermoelastic media based on a memory-dependent generalized thermoelastic theory.

In this paper, thermal contact resistance and elastic wave impedance are considered to simulate the imperfect conditions at the interface of a bilayered saturated porous media. The fractional derivative theory of thermoelasticity is introduced to describe the thermodynamic behavior of a bilayered saturated porous media. The analytical solutions of the dynamic response of the bilayered saturated porous media are derived by applying the operator decomposition method. Using the derived solutions, the effects of the fractional derivative parameters and thermal contact resistance on the dynamic response of bilayered saturated porous media are discussed in detail.

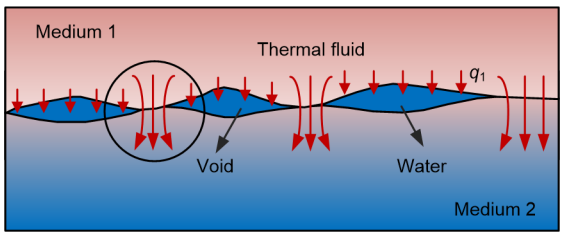

Fig. 1 Thermal contact resistance model
q_1 represents the heat flux

2 Problem formulation and governing equations

A schematic of a bilayered saturated porous media composed of two kinds of isotropic and homogeneous saturated porous media with different properties is shown in Fig. 2. The first layer is marked by 1 and the second layer by 2. The upper part of the saturated porous media is subjected to a uniform harmonic temperature load $\theta_0 e^{i\omega t}$, where the angular frequency is denoted by ω and the temperature constant by θ_0. i denotes a complex number, $i^2=-1$, e the exponential function, and t the time. The model does not incorporate any external force or free drainage boundaries. The saturated porous media 1 and 2 are not in complete contact because of the presence of tiny pores. Moreover, the pores contain a small amount of water. The thermal impedance and the reflection and transmission propagation characteristics of elastic waves at the interface between the two layers ($x=h$) are taken into consideration, where

h is the thickness of the first layer and x is the coordinate of an origin at top surface (Fig. 2). The lower part of medium 2 is infinite, i.e. it satisfies the condition $x\to\infty$. Both the pore water pressure and displacement are fixed at 0, and the temperature remains unchanged.

As shown in Fig. 2, the corresponding boundary conditions are derived as:

$$\sigma_1(0,t)=0, \tag{1}$$

$$\theta_1(0,t)=\theta_0 e^{i\omega t}, \tag{2}$$

$$u_2(x\to\infty,t)=0, \tag{3}$$

$$\theta_2(x\to\infty,t)=0, \tag{4}$$

$$p_{f2}(x\to\infty,t)=0, \tag{5}$$

$$p_{f1}(0,t)=0. \tag{6}$$

The interfacial conditions (Xue et al., 2016) are introduced as:

$$q_1(h,t)=hm\left[\theta_1(h,t)-\theta_2(h,t)\right], \tag{7}$$

$$q_1(h,t)=q_2(h,t), \tag{8}$$

$$u_1(h,t)=u_2(h,t), \tag{9}$$

$$\frac{\sigma_2(h,t)}{\sigma_1(h,t)}=\frac{2}{1+Z_1/Z_2}, \tag{10}$$

$$p_{f1}(h,t)=p_{f2}(h,t), \tag{11}$$

where σ_j (j=1, 2, unless otherwise stated) denotes the stress; $\theta_j=T-T_0$ represents the temperature increment; T and T_0 are the absolute and reference temperatures, respectively; u_j denotes the displacement; q_j represents the heat flux; p_{fj} denotes the pore water pressure; m denotes the film coefficient at the interface; Z_1 and Z_2 are the elastic wave impedances for layers 1 and 2, respectively. Furthermore, Z_1 and Z_2 can be obtained as $Z_1=\rho_1c_1=\sqrt{(\lambda_1+2\mu_1)\rho_1}$ and $Z_2=\rho_2c_2=\sqrt{(\lambda_2+2\mu_2)\rho_2}$, respectively. λ_j is the Lame constant; μ_j denotes the shear modulus; c_j depicts the longitudinal wave velocity of the porous media; $\rho_j=n_j\rho_{fj}+(1-n_j)\rho_{sj}$ represents the density of the porous media; ρ_{fj} denotes the density of the pore water; ρ_{sj} denotes the density of the solid grains; n_j is the porosity.

Ezzat et al. (2015) proposed a fractional derivative heat conduction equation:

$$q_j+\frac{\tau_j^{\alpha_j}}{\alpha_j!}\frac{\partial^{\alpha_j}q_j}{\partial t^{\alpha_j}}=-k_j\frac{\partial\theta_j}{\partial x}, \tag{12}$$

where α_j denotes the fractional derivative parameter, τ_j denotes the relaxation time, and k_j denotes the heat conduction coefficient.

The governing equation for temperature is given as:

$$m_j\left(1+\frac{\tau_j^{\alpha_j}}{\alpha_j!}\frac{\partial^{\alpha_j}}{\partial t^{\alpha_j}}\right)\frac{\partial\theta_j}{\partial t}+\beta_jT_0\left(1+\frac{\tau_j^{\alpha_j}}{\alpha_j!}\frac{\partial^{\alpha_j}}{\partial t^{\alpha_j}}\right)\frac{\partial e_j}{\partial t}=k_j\frac{\partial^2\theta_j}{\partial x^2}, \tag{13}$$

where $\beta_j=(3\lambda_j+2\mu_j)\alpha_{sj}$ denotes the thermoelastic modulus; α_{sj} represents the linear thermal expansion coefficient of solid grains; $m_j=n_j\rho_{fj}c_{fj}+(1-n_j)\rho_{sj}c_{sj}$ is the volumetric heat capacity of the media in which c_{fj} and c_{sj} are the specific heat at constant strain of pore

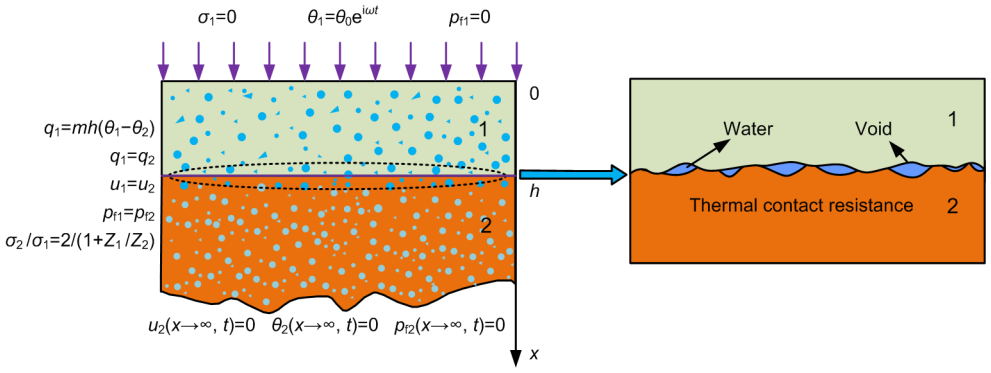

Fig. 2 Schematic of the bilayered saturated porous media

water and solid grains, respectively; $e_j=\partial u_j/\partial x$ is the volumetric strain. As shown in Fig. 2, by neglecting the inertial effect and body force of the fluid, the motion equation of the bilayered saturated porous media can be written as (Lu et al., 2010):

$$\frac{\partial \sigma_j}{\partial x}=\rho_j\frac{\partial^2 u_j}{\partial t^2}. \tag{14}$$

The constitutive relation can be written as (Ai and Wang, 2015a):

$$\sigma_j=(\lambda_j+2\mu_j)e_j-\beta_j\theta_j-p_{\mathrm{f}j}. \tag{15}$$

According to Darcy's law, the fluid motion equation can be expressed as (Lu et al., 2010):

$$b_j\frac{\partial}{\partial t}\left(\alpha_{\mathrm{f}j}\theta_j-e_j\right)+\rho_{\mathrm{f}j}\frac{\partial^2 e_j}{\partial t^2}+\frac{\partial^2 p_{\mathrm{f}j}}{\partial x^2}=0, \tag{16}$$

where $b_j=\rho_{\mathrm{f}j}g/k_{\mathrm{d}j}$; g is the gravitational acceleration; $k_{\mathrm{d}j}$ is the permeability coefficient of the porous media; $\alpha_{\mathrm{f}j}$ is the coefficient of linear thermal expansion of pore water.

Substituting Eq. (15) into Eq. (14), the motion equation in terms of displacement can be obtained as:

$$(\lambda_j+2\mu_j)\frac{\partial^2 u_j}{\partial x^2}-\beta_j\frac{\partial\theta_j}{\partial x}-\frac{\partial p_{\mathrm{f}j}}{\partial x}=\rho_j\frac{\partial^2 u_j}{\partial t^2}. \tag{17}$$

3 Solutions to governing equations

To solve Eqs. (12)–(17), the following dimensionless quantities are introduced:

$$x^*=\xi_1\xi_2 x,\ t^*=\xi_1{}^2\xi_2 t,\ \tau_j{}^*=\xi_1{}^2\xi_2\tau_j,\ \sigma_j{}^*=\sigma_j/\mu_1,$$
$$\theta_j{}^*=\theta_j/T_0,\ q_j{}^*=q_j/(k_1T_0\xi_1\xi_2),\ p_{\mathrm{f}j}{}^*=p_{\mathrm{f}j}/\mu_1,$$

where $\xi_1=[(\lambda_1+2\mu_1)/\rho_1]^{1/2}$ and $\xi_2=m_1/k_1$. In the dimensionless form, the governing Eqs. (12), (13), and (15)–(17) can be rewritten as:

$$\left(1+\frac{\tau_j^{\alpha_j}}{\alpha_j!}\frac{\partial^{\alpha_j}}{\partial t^{\alpha_j}}\right)q_j=-\frac{k_j}{k_1}\frac{\partial\theta_j}{\partial x},\ 0<\alpha_j\le 1, \tag{18}$$

$$\sigma_j=\frac{\lambda_j+2\mu_j}{\mu_1}e_j-\frac{\beta_jT_0}{\mu_1}\theta_j-p_{\mathrm{f}j}, \tag{19}$$

$$\frac{\lambda_j+2\mu_j}{\rho_j\xi_1^2}\frac{\partial^2 u_j}{\partial x^2}-\frac{\beta_jT_0}{\rho_j\xi_1^2}\frac{\partial\theta_j}{\partial x}-\frac{\mu_1}{\rho_j\xi_1^2}\frac{\partial p_{\mathrm{f}j}}{\partial x}=\frac{\partial^2 u_j}{\partial t^2}, \tag{20}$$

$$\begin{aligned}&\frac{m_j}{k_j\xi_2}\left(1+\frac{\tau_j^{\alpha_j}}{\alpha_j!}\frac{\partial^{\alpha_j}}{\partial t^{\alpha_j}}\right)\frac{\partial\theta_j}{\partial t}\\&\quad+\frac{\beta_j}{k_j\xi_2}\left(1+\frac{\tau_j^{\alpha_j}}{\alpha_j!}\frac{\partial^{\alpha_j}}{\partial t^{\alpha_j}}\right)\frac{\partial e_j}{\partial t}=\frac{\partial^2\theta_j}{\partial x^2},\end{aligned} \tag{21}$$

$$\frac{b_j}{\mu_1\xi_2}\frac{\partial}{\partial t}\left(\alpha_{\mathrm{f}j}T_0\theta_j-e_j\right)+\frac{\rho_{\mathrm{f}j}\xi_1^2}{\mu_1}\frac{\partial^2 e_j}{\partial t^2}+\frac{\partial^2 p_{\mathrm{f}j}}{\partial x^2}=0. \tag{22}$$

After multiplying $\partial/\partial x$ on both sides, Eq. (20) can be rewritten as:

$$\frac{\lambda_j+2\mu_j}{\rho_j\xi_1^2}\frac{\partial^2 e_j}{\partial x^2}-\frac{\beta_jT_0}{\rho_j\xi_1^2}\frac{\partial^2\theta_j}{\partial x^2}-\frac{\mu_1}{\rho_j\xi_1^2}\frac{\partial^2 p_{\mathrm{f}j}}{\partial x^2}=\frac{\partial^2 e_j}{\partial t^2}. \tag{23}$$

Combining Eqs. (22) and (23), the following expression can be derived:

$$\begin{aligned}&\frac{\lambda_j+2\mu_j}{\rho_j\xi_1^2}\frac{\partial^2 e_j}{\partial x^2}-\frac{\beta_jT_0}{\rho_j\xi_1^2}\frac{\partial^2\theta_j}{\partial x^2}\\&\quad+\frac{b_j}{\rho_j\xi_1^2\xi_2}\frac{\partial}{\partial t}\left(\alpha_{\mathrm{f}j}T_0\theta_j-e_j\right)=\frac{\partial^2 e_j}{\partial t^2}\left(1-\frac{\rho_{\mathrm{f}j}}{\rho_j}\right).\end{aligned} \tag{24}$$

For steady-state vibration with an angular frequency of ω, Eqs. (24) and (21) can be respectively rewritten as:

$$\begin{aligned}&\frac{\lambda_j+2\mu_j}{\rho_j\xi_1^2}\frac{\partial^2 e_j}{\partial x^2}-\frac{\beta_jT_0}{\rho_j\xi_1^2}\frac{\partial^2\theta_j}{\partial x^2}\\&\quad+\frac{b_j\mathrm{i}\omega}{\rho_j\xi_1^2\xi_2}\left(\alpha_{\mathrm{f}j}T_0\theta_j-e_j\right)-\frac{\rho_{\mathrm{f}j}\omega^2}{\rho_j}e_j+\omega^2 e_j=0,\end{aligned} \tag{25}$$

$$\begin{aligned}&\frac{m_j\mathrm{i}\omega}{k_j\xi_2}\left(1+\frac{\tau_j^{\alpha_j}(\mathrm{i}\omega)^{\alpha_j}}{\alpha_j!}\right)\theta_j\\&\quad+\frac{\beta_j\mathrm{i}\omega}{k_j\xi_2}\left(1+\frac{\tau_j^{\alpha_j}(\mathrm{i}\omega)^{\alpha_j}}{\alpha_j!}\right)e_j=\frac{\partial^2\theta_j}{\partial x^2}.\end{aligned} \tag{26}$$

The analytic solutions of dynamic response of bilayered saturated porous media are obtained by Eqs. (19), (25), and (26), and the analytic expressions of temperature increment, displacement, pore water pressure, and stress are also obtained. So the problem may be completely solved. The solving process is neglected here and the reader is referred to electronic supplementary materials for detailed derivation.

4 Results and discussion

In this section, the effects of the fractional derivative parameters α_1 and α_2, and the thermal contact resistance X_T on the temperature increment, displacement, pore water pressure, and stress of a layered saturated porous media are systematically evaluated. Non-dimensional relaxation times of $\tau_1=\tau_2=0.5$ are adopted and the non-dimensional thickness of saturated porous medium 1 is set as $h=0.5$. The non-dimensional frequency is set as $\omega=0.5$, and the elastic wave impedance ratio is given as $Z_1/Z_2=1.0$. The material constants of saturated soil, which are assigned to saturated porous media 1 and 2, are shown in Table 1 (Lu et al., 2010; Wen et al., 2020). In addition, $T_0=293$ K and $\theta_0=1$.

4.1 Comparison and validation

First, the rationality and accuracy of the present solutions were verified by comparison with an existing solution. When $X_T=10^{-10}$ and $Z_1/Z_2=1.0$, the boundary conditions of this study, i.e. $X_T\left.\frac{\partial\theta_1}{\partial x}\right|_{x=h}=-\left[1+\frac{\tau_1^{\alpha_1}}{\alpha_1!}(\mathrm{i}\omega)^{\alpha_1}\right]\left(\theta_1|_{x=h}-\theta_2|_{x=h}\right)$ and $\frac{\sigma_2|_{x=h}}{\sigma_1|_{x=h}}=\frac{2}{1+Z_1/Z_2}$, can be degraded into the continuous boundary conditions at the interface of the bilayered saturated porous media ($x=h=0.5$).

When $n_1=n_2=0$ and $\rho_{f1}=0$, the porous thermoelastic media in this study can be degraded into a thermoelastic solid. Therefore, replacing s (s denotes the complex variable in the Laplace domain) with $\mathrm{i}\omega$ in the solution of Xue et al. (2016), the problem of Xue et al. (2016) can be degraded into the dynamic response problem of a bilayered thermoelastic media under harmonic thermal load. To validate the accuracy of the proposed solutions, the present results were compared with those reported by Xue et al. (2016). Fig. 3 demonstrates the variations of temperature increment and displacement with the depth x. The present results are generally consistent with those of Xue et al. (2016). When $X_T=10^{-10}$, the interface ($x=0.5$) is degraded into the continuity condition, i.e. $x=0.5$. At this time, the thermal wave passes through the first layer and then completely reflects to the second layer of the thermoelastic media via the interface. At $x=0.5$, the thermal gradient at the interface exhibits a jumping phenomenon, which becomes even more obvious with the increase of X_T.

Table 1 Default parameters adopted in the parametric study (Lu et al., 2010; Wen et al., 2020)

Variable	Value	
	Layer 1	Layer 2
Lame constant, λ (Pa)	4×10^6	6×10^6
Shear modulus, μ (Pa)	1×10^6	2×10^6
Solid grains density, ρ_s (kg/m^3)	2600	1000
Thermal conductivity, k (J/(s·m·°C))	4	2
Thermal expansion coefficient of solid grains, α_s	3.0×10^{-5}	4.5×10^{-5}
Thermal expansion coefficient of fluid, α_f (°C^{-1})	3.00×10^{-4}	2.25×10^{-4}
Specific heat of solid grains, c_s (J/(kg·°C))	2000	1500
Specific heat of fluid, c_{f1} (J/(kg·°C))	4000	4000
Porosity, n	0.4	0.4
Fluid-solid coupling coefficient, b	100	100

4.2 Effects of fractional derivative parameters

Fig. 4 shows the effects of the fractional derivative parameters α_1 and α_2 on the temperature increment, displacement, pore water pressure, and stress of the bilayered saturated porous media, when $X_T=10^{-10}$ and $Z_1/Z_2=1.0$. When $\alpha_1=\alpha_2=0.25$, the heat conduction is weak, which results in relatively small magnitudes of temperature increment, displacement, pore water pressure, and stress. With the increase of α_1 and α_2, the magnitude of the responses of these parameters increases significantly. On the other hand, when $\alpha_1=\alpha_2=1.0$, the heat conduction is strong.

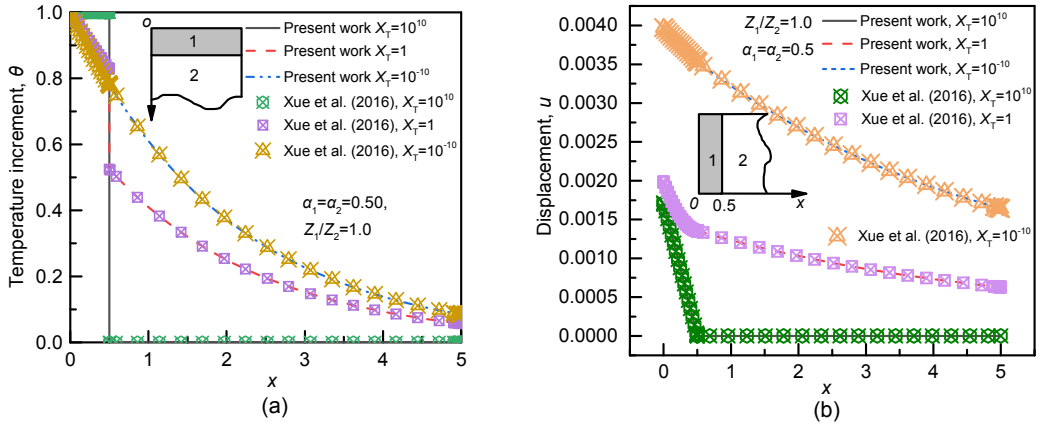

Fig. 3 Comparison between the results of the present method and those reported by Xue et al. (2016)
(a) Temperature increment; (b) Displacement

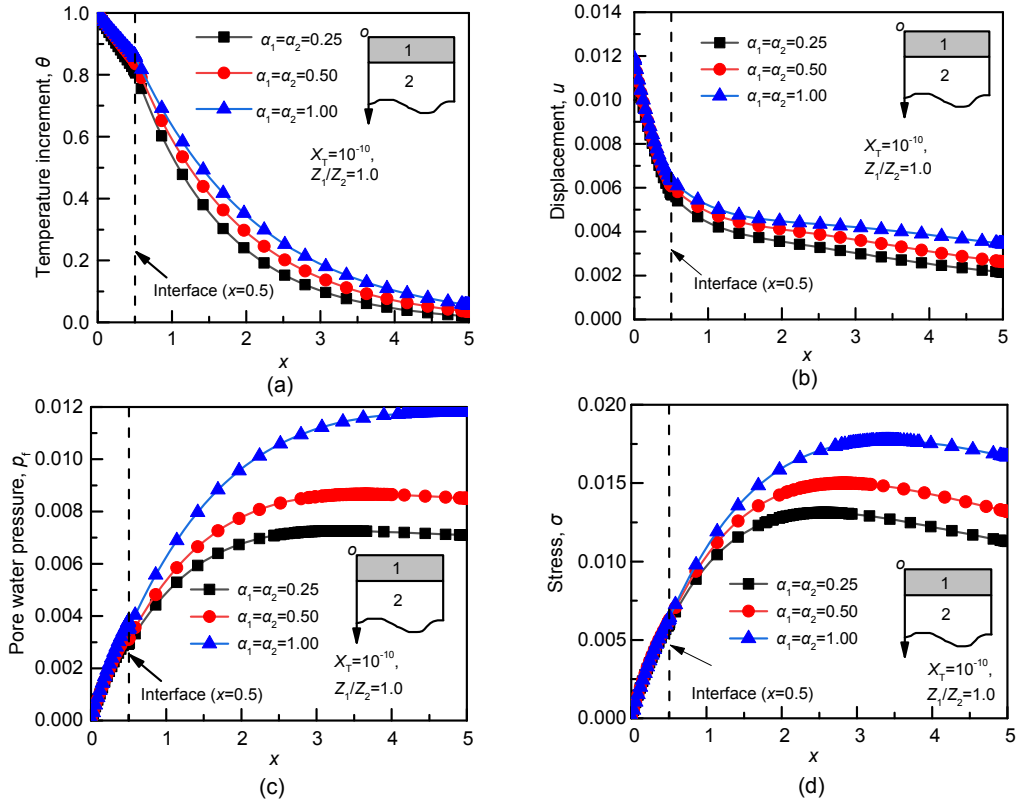

Fig. 4 Effects of fractional derivative parameters on temperature increment (a), displacement (b), pore water pressure (c), and stress (d), when X_T=10^{-10} and Z_1/Z_2=1.0

Fig. 5 shows the effects of the fractional derivative parameters α_1 and α_2 on the temperature increment, displacement, pore water pressure, and stress of the bilayered saturated porous media when there is thermal contact resistance at the interface of the two layers (X_T=1 and Z_1/Z_2=1.0). For the temperature increment, a sudden leap can be observed at the interface (x=h). The temperature of the second layer is significantly lower than that close to the continuous boundary (X_T=10^{-10}), and is accompanied by rapid attenuation. As the fractional derivative parameters α_1 and α_2 increase, the magnitudes of the responses

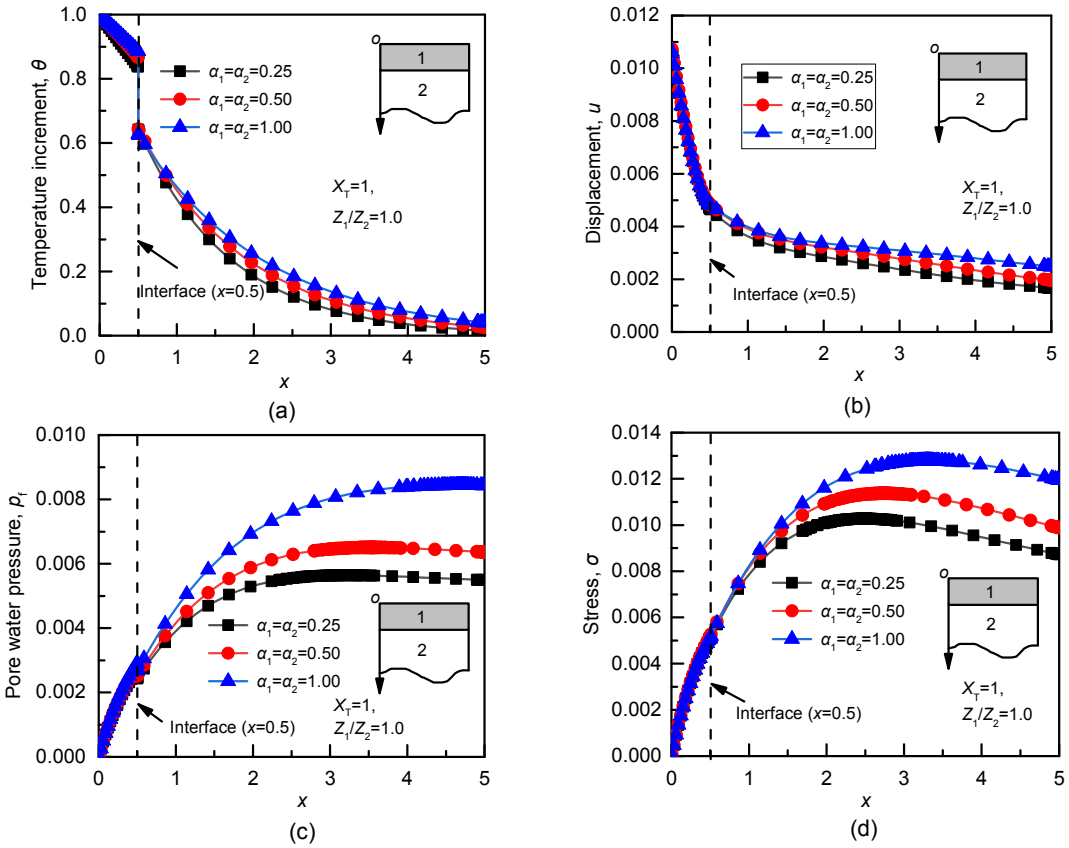

Fig. 5 Effects of fractional derivative parameters on temperature increment (a), displacement (b), pore water pressure (c), and stress (d), when X_T=1 and Z_1/Z_2=1.0

of the second layer increase significantly. However, they are significantly lower than those close to the continuous boundary (X_T=10^{-10}). This can be attributed to the existence of a gap at the interface, because there is a small amount of water in the gap, and the thermal conductivity of water is much lower than that of saturated porous media.

Fig. 6 demonstrates the effects of the fractional derivative parameter α_1 on the temperature increment, displacement, pore water pressure, and stress of a bilayered saturated porous media under complete contact at the interface of the two layers (X_T=10^{-10}) when α_2=1.0 and Z_1/Z_2=1.0. The fractional derivative parameter α_1 of the first layer can significantly affect the temperature increment, displacement, pore water pressure, and stress of the second layer. With the increase of α_1, the temperature increment, displacement, pore water pressure, and stress increase in magnitude. This can be attributed to the enhancement of the strength of heat conduction with increasing α_1.

Fig. 7 shows the effects of the fractional derivative parameter α_2 on the temperature increment, displacement, pore water pressure, and stress of the bilayered saturated porous media under complete contact at the interface of the two layers (X_T=10^{-10}) when α_1=1.0 and Z_1/Z_2=1.0. The fractional derivative parameter α_2 has a more significant effect than α_1 on the dynamic thermoelastic response of the bilayered saturated porous media. With the increase of α_2, the magnitudes of the responses of the second layer parameters, and especially those of pore water pressure and stress, increase gradually. We can conclude that the fractional derivative parameters α_1 and α_2 can adequately describe the THM coupling behavior of the saturated porous media.

4.3 Effects of thermal contact resistance

Fig. 8 (p.1001) shows the effect of thermal contact resistance on the temperature increment, displacement, pore water pressure, and stress of the bilayered saturated porous media, when α_1=α_2=0.5 and Z_1/Z_2=1.0.

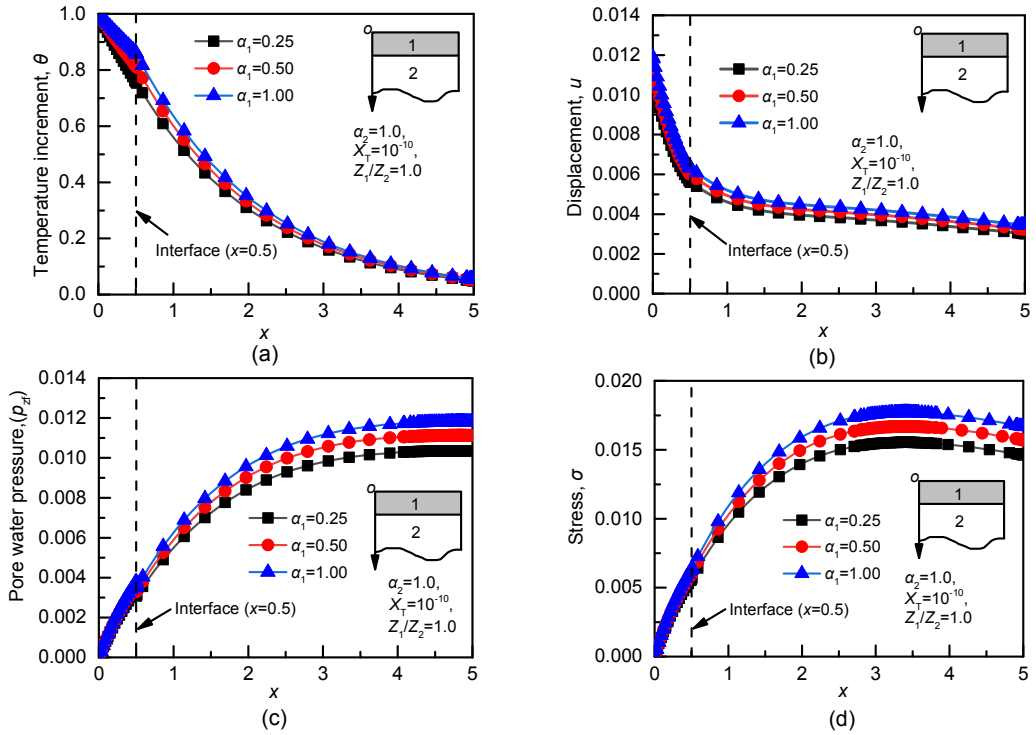

Fig. 6 Effects of fractional derivative parameter α_1 on temperature increment (a), displacement (b), pore water pressure (c), and stress (d), when $X_T=10^{-10}$, $Z_1/Z_2=1.0$, and $\alpha_2=1.0$

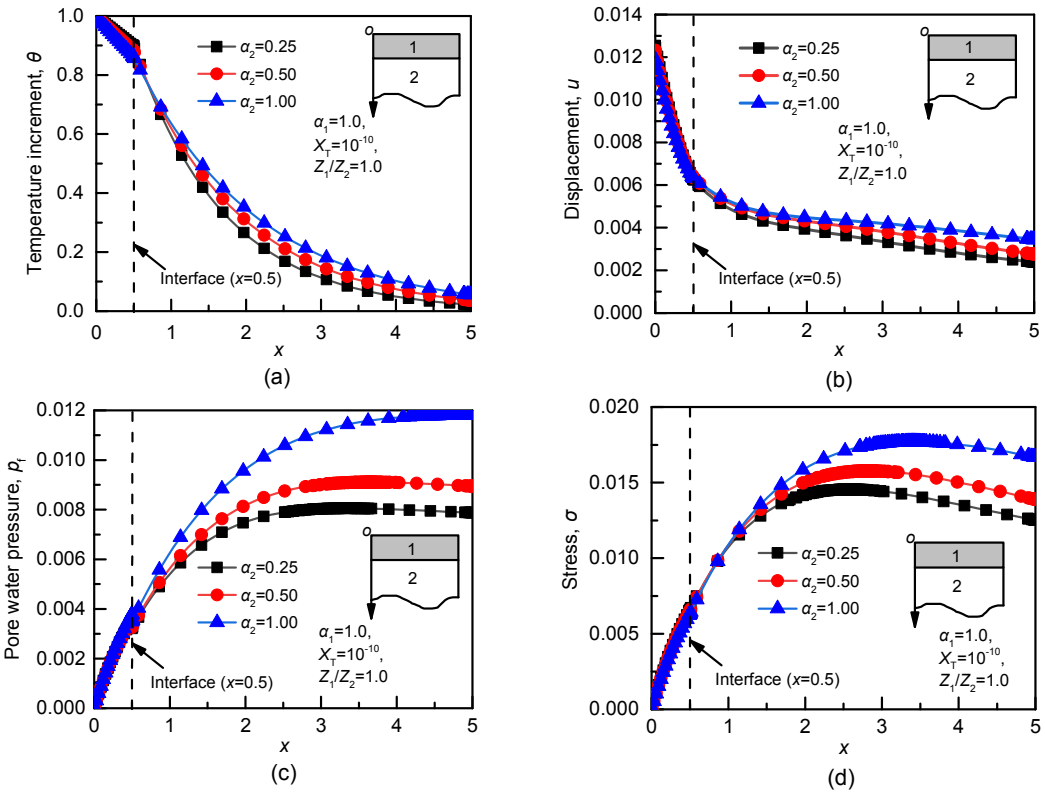

Fig. 7 Effects of fractional derivative parameter α_2 on temperature increment (a), displacement (b), pore water pressure (c), and stress (d), when $X_T=10^{-10}$, $Z_1/Z_2=1.0$, and $\alpha_1=1.0$

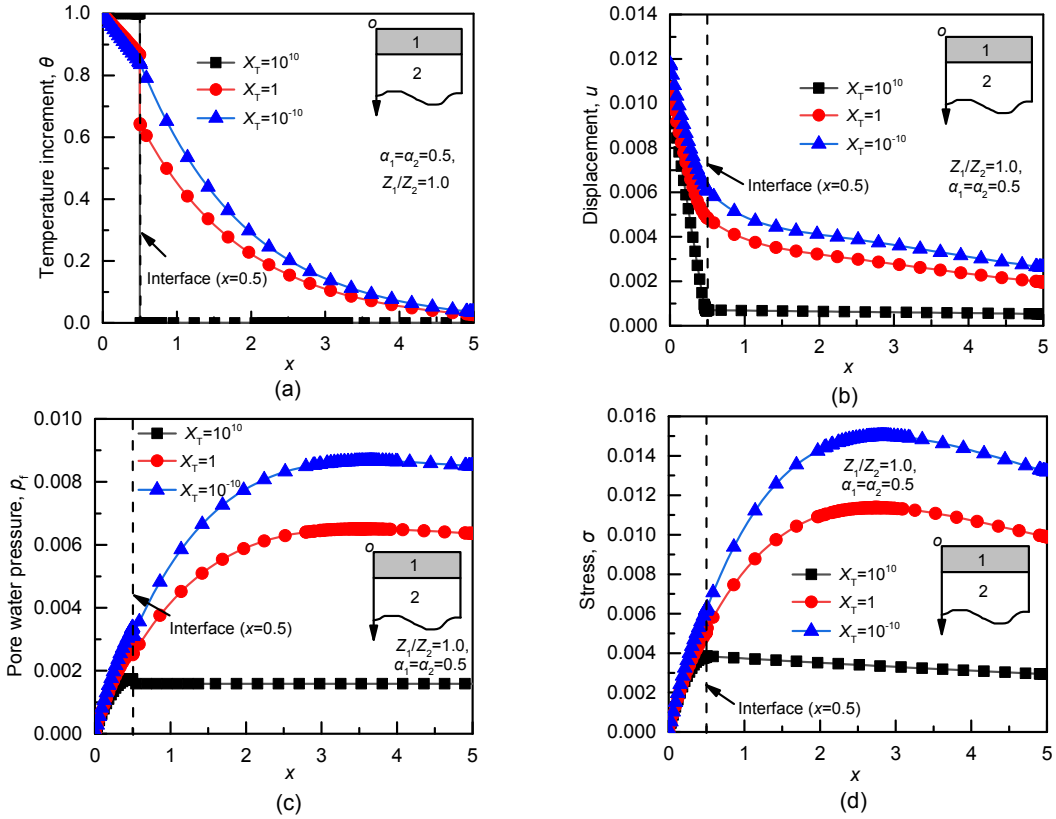

Fig. 8 Effects of thermal contact resistance X_T on temperature increment (a), displacement (b), pore water pressure (c), and stress (d), when $\alpha_1=\alpha_2=0.5$ and $Z_1/Z_2=1.0$

According to Fig. 8a, for $X_T=10^{10}$, the interface of the bilayered saturated porous media ($x=h$) is similar to that of a complete insulation condition, under which the heat wave can be completely reflected to the first layer when it passes through the interface. Therefore, the temperature increments in the first and second layers are close to 1 and 0, respectively. For $X_T=1$, part of the heat wave enters the second layer through the interface, while another part is reflected, resulting in a sudden incremental leap in temperature at the interface. For $X_T=10^{10}$, the interface is close to the continuous boundary condition, and the heat wave can be fully transmitted to the second layer; thus, the temperature increment forms a smooth curve. In Fig. 8b, for $X_T=10^{10}$, the displacement of the second layer is almost equal to 0. This is because the temperature increment in the second layer is almost equal to 0, since most of the heat is reflected to the first layer. For $X_T=10^{-10}$, the contact surface satisfies the continuous boundary condition, and the heat can be completely transmitted to the second layer, producing great deformation between the two layers. As shown in Figs. 8c and 8d, the pore water pressure and stress increase significantly with the decrease in the thermal contact resistance. When the contact surface approaches the insulation condition ($X_T=10^{-10}$), the heat can be transmitted to the second layer after passing through the interface. Accordingly, the second layer exhibits a great temperature increase, accompanied by an increase in the pore water pressure and stress in the two layers.

5 Conclusions

In this paper, a fractional derivative THM coupling thermoelastic model of saturated porous media is developed based on fractional thermoelastic theory and the poroelastic wave equation. The thermal contact resistance and the elastic wave impedance at the interface are introduced to analyze the THM coupling dynamic response of a bilayered saturated porous media. After analyzing the effects of the fractional derivative parameters and thermal contact

resistance on the dynamic response of the bilayered saturated porous media, the following conclusions could be drawn:

1. With the increase of the fractional derivative parameters α_1 and α_2, the response amplitudes of the temperature increment, displacement, pore water pressure, and stress increase significantly. Moreover, the effect of fractional derivative parameters on the THM coupling response is related to the thermal contact resistance at the interface. If there is thermal contact resistance at the interface, the effect of the fractional derivative parameters on the system response is weakened. The fractional derivative parameters can reveal the heat conduction intensity and thermodynamic behavior of the THM coupling response of a bilayered saturated porous media.

2. The effect of the fractional derivative parameter α_2 on the temperature increment, displacement, and pore water pressure of a bilayered saturated porous media is stronger than that of α_1. Furthermore, the response amplitudes of the second layer increase steadily as the fractional derivative parameter α_2 increases.

3. Because of thermal contact resistance at the interface, the temperature increment at the interface exhibits a jumping phenomenon, which becomes more obvious as the thermal contact resistance increases. With the increase of thermal contact resistance, the displacement, pore water pressure, and stress at the interface decrease gradually.

Contributors

Min-jie WEN designed the research. Min-jie WEN and Kui-hua WANG processed the corresponding data. Min-jie WEN wrote the first draft of the manuscript. Wen-bing WU and Yun-peng ZHANG helped to organize the manuscript. Hou-ren XIONG revised and edited the final version.

Conflict of interest

Min-jie WEN, Kui-hua WANG, Wen-bing WU, Yun-peng ZHANG, and Hou-ren XIONG declare that they have no conflict of interest.

References

Abbas IA, Marin M, 2018. Analytical solutions of a two-dimensional generalized thermoelastic diffusions problem due to laser pulse. *Iranian Journal of Science and Technology, Transactions of Mechanical Engineering*, 42(1):57-71. https://doi.org/10.1007/s40997-017-0077-1

Abbas IA, Alzahrani FS, Elaiw A, 2019. A DPL model of photothermal interaction in a semiconductor material. *Waves in Random and Complex Media*, 29(2):328-343. https://doi.org/10.1080/17455030.2018.1433901

Ai ZY, Wang LJ, 2015a. Axisymmetric thermal consolidation of multilayered porous thermoelastic media due to a heat source. *International Journal for Numerical and Analytical Methods in Geomechanics*, 39(17):1912-1931. https://doi.org/10.1002/nag.2381

Ai ZY, Wang LJ, 2015b. Time-dependent analysis of 3D thermo-mechanical behavior of a layered half-space with anisotropic thermal diffusivity. *Acta Mechanica*, 226(9): 2939-2954. https://doi.org/10.1007/s00707-015-1360-0

Ai ZY, Wang LJ, 2016. Three-dimensional thermo-hydro-mechanical responses of stratified saturated porothermoelastic material. *Applied Mathematical Modelling*, 40(21-22):8912-8933. https://doi.org/10.1016/j.apm.2016.05.034

Ai ZY, Ye Z, Zhao Z, et al., 2018. Time-dependent behavior of axisymmetric thermal consolidation for multilayered transversely isotropic poroelastic material. *Applied Mathematical Modelling*, 61:216-236. https://doi.org/10.1016/j.apm.2018.04.012

Alzahrani F, Abbas IA, 2020. Generalized thermoelastic interactions in a poroelastic material without energy dissipations. *International Journal of Thermophysics*, 41(7): 95. https://doi.org/10.1007/s10765-020-02673-0

Alzahrani F, Hobiny A, Abbas I, et al., 2020. An eigenvalues approach for a two-dimensional porous medium based upon weak, normal and strong thermal conductivities. *Symmetry*, 12(5):848. https://doi.org/10.3390/sym12050848

Bhatti MM, Marin M, Zeeshan A, et al., 2020. Swimming of motile gyrotactic microorganisms and nanoparticles in blood flow through anisotropically tapered arteries. *Frontiers in Physics*, 8:95. https://doi.org/10.3389/fphy.2020.00095

Biot MA, 1956. Thermoelasticity and irreversible thermodynamics. *Journal of Applied Physics*, 27(3):240-253. https://doi.org/10.1063/1.1722351

Booker JR, Savvidou C, 1984. Consolidation around a spherical heat source. *International Journal of Solids and Structures*, 20(11-12):1079-1090. https://doi.org/10.1016/0020-7683(84)90091-X

Carr EJ, March NG, 2018. Semi-analytical solution of multilayer diffusion problems with time-varying boundary conditions and general interface conditions. *Applied Mathematics and Computation*, 333:286-303. https://doi.org/10.1016/j.amc.2018.03.095

Deswal S, Kalkal KK, 2013. Fractional order heat conduction law in micropolar thermo-viscoelasticity with two temperatures. *International Journal of Heat and Mass Transfer*, 66:451-460. https://doi.org/10.1016/j.ijheatmasstransfer.2013.07.047

Ezzat MA, El-Karamany AS, El-Bary AA, 2015. On thermo-viscoelasticity with variable thermal conductivity and fractional-order heat transfer. *International Journal of Thermophysics*, 36(7):1684-1697. https://doi.org/10.1007/s10765-015-1873-8

Green AE, Lindsay KA, 1972. Thermoelasticity. *Journal of Elasticity*, 2(1):1-7. https://doi.org/10.1007/BF00045689

He TH, Zhang P, Xu C, et al., 2019. Transient response analysis of a spherical shell embedded in an infinite thermoelastic medium based on a memory-dependent generalized thermoelasticity. *Journal of Thermal Stresses*, 42(8):943-961. https://doi.org/10.1080/01495739.2019.1610342

Hobiny A, Abbas I, 2020. Fractional order GN model on photo-thermal interaction in a semiconductor plane. *Silicon*, 12(8):1957-1964. https://doi.org/10.1007/s12633-019-00292-5

Hobiny A, Abbas I, 2021. Analytical solutions of fractional bioheat model in a spherical tissue. *Mechanics Based Design of Structures and Machines*, 49(3):430-439. https://doi.org/10.1080/15397734.2019.1702055

Hussein EM, 2015. Fractional order thermoelastic problem for an infinitely long solid circular cylinder. *Journal of Thermal Stresses*, 38(2):133-145. https://doi.org/10.1080/01495739.2014.936253

Hussein EM, 2018. Effect of the porosity on a porous plate saturated with a liquid and subjected to a sudden change in temperature. *Acta Mechanica*, 229(6):2431-2444. https://doi.org/10.1007/s00707-017-2106-y

Kek-Kiong T, Sadhal SS, 1992. Thermal constriction resistance: effects of boundary conditions and contact geometries. *International Journal of Heat and Mass Transfer*, 35(6):1533-1544. https://doi.org/10.1016/0017-9310(92)90043-R

Khan AA, Bukhari SR, Marin M, et al., 2019. Effects of chemical reaction on third-grade MHD fluid flow under the influence of heat and mass transfer with variable reactive index. *Heat Transfer Research*, 50(11):1061-1080. https://doi.org/10.1615/HeatTransRes.2018028397

Levy A, Sorek S, Ben-Dor G, et al., 1995. Evolution of the balance equations in saturated thermoelastic porous media following abrupt simultaneous changes in pressure and temperature. *Transport in Porous Media*, 21(3):241-268. https://doi.org/10.1007/BF00617408

Li CL, Tian XG, He TH, 2020. Transient thermomechanical responses of multilayered viscoelastic composite structure with non-idealized interfacial conditions in the context of generalized thermoviscoelasticity theory with time-fractional order strain. *Journal of Thermal Stresses*, 43(7):895-928. https://doi.org/10.1080/01495739.2020.1751760

Li CX, Xie KH, 2013. One-dimensional nonlinear consolidation of soft clay with the non-Darcian flow. *Journal of Zhejiang University-SCIENCE A (Applied Physics & Engineering)*, 14(6):435-446. https://doi.org/10.1631/jzus.A1200343

Li CX, Xie KH, Wang K, 2010. Analysis of 1D consolidation with non-Darcian flow described by exponent and threshold gradient. *Journal of Zhejiang University-SCIENCE A (Applied Physics & Engineering)*, 11(9):656-667. https://doi.org/10.1631/jzus.A0900787

Li CX, Xie KH, Hu AF, et al., 2012. One-dimensional consolidation of double-layered soil with non-Darcian flow described by exponent and threshold gradient. *Journal of Central South University*, 19(2):562-571. https://doi.org/10.1007/s11771-012-1040-3

Li CX, Wang CJ, Lu MM, et al., 2017. One-dimensional large-strain consolidation of soft clay with non-Darcian flow and nonlinear compression and permeability of soil. *Journal of Central South University*, 24(4):967-976. https://doi.org/10.1007/s11771-017-3499-4

Li CX, Xiao JY, Wu WB, et al., 2020. Analysis of 1D large strain consolidation of structured marine soft clays. *Journal of Zhejiang University-SCIENCE A (Applied Physics & Engineering)*, 21(1):29-43. https://doi.org/10.1631/jzus.A1900268

Liu GB, Xie KH, Zheng RY, 2009. Model of nonlinear coupled thermo-hydro-elastodynamics response for a saturated poroelastic medium. *Science in China Series E: Technological Sciences*, 52(8):2373-2383. https://doi.org/10.1007/s11431-008-0220-8

Liu GB, Liu XH, Ye RH, 2010a. The relaxation effects of a saturated porous media using the generalized thermoviscoelasticity theory. *International Journal of Engineering Science*, 48(9):795-808. https://doi.org/10.1016/j.ijengsci.2010.04.006

Liu GB, Xie KH, Zheng RY, 2010b. Thermo-elastodynamic response of a spherical cavity in saturated poroelastic medium. *Applied Mathematical Modelling*, 34(8):2203-2222. https://doi.org/10.1016/j.apm.2009.10.031

Lord HW, Shulman Y, 1967. A generalized dynamical theory of thermoelasticity. *Journal of the Mechanics and Physics of Solids*, 15(5):299-309. https://doi.org/10.1016/0022-5096(67)90024-5

Lu Z, Yao HL, Liu GB, 2010. Thermomechanical response of a poroelastic half-space soil medium subjected to time harmonic loads. *Computers and Geotechnics*, 37(3):343-350. https://doi.org/10.1016/j.compgeo.2009.11.007

Mei GX, Yin JH, 2008. Coupled model of consolidation and creep for consolidation test. *Journal of Central South University*, 15(S1):357-361. https://doi.org/10.1007/s11771-008-0380-5

Mei GX, Chen QM, 2013. Solution of Terzaghi one-dimensional consolidation equation with general boundary conditions. *Journal of Central South University*, 20(8):2239-2244.

https://doi.org/10.1007/s11771-013-1730-5

Peng W, Ma YB, Li CL, et al., 2020. Dynamic analysis to the fractional order thermoelastic diffusion problem of an infinite body with a spherical cavity and variable material properties. *Journal of Thermal Stresses*, 43(1):38-54. https://doi.org/10.1080/01495739.2019.1676681

Saeed T, Abbas I, Marin M, 2020. A GL model on thermoelastic interaction in a poroelastic material using finite element method. *Symmetry*, 12(3):488. https://doi.org/10.3390/sym12030488

Sherief HH, Hussein EM, 2012. A mathematical model for short-time filtration in poroelastic media with thermal relaxation and two temperatures. *Transport in Porous Media*, 91(1):199-223. https://doi.org/10.1007/s11242-011-9840-8

Sherief HH, El-Latief AMA, 2013. Effect of variable thermal conductivity on a half-space under the fractional order theory of thermoelasticity. *International Journal of Mechanical Sciences*, 74:185-189. https://doi.org/10.1016/j.ijmecsci.2013.05.016

Sherief HH, El-Sayed AMA, El-Latief AMA, 2010. Fractional order theory of thermoelasticity. *International Journal of Solids and Structures*, 47(2):269-275. https://doi.org/10.1016/j.ijsolstr.2009.09.034

Sherief HH, El-Latief AMA, 2015. A one-dimensional fractional order thermoelastic problem for a spherical cavity. *Mathematics and Mechanics of Solids*, 20(5):512-521. https://doi.org/10.1177/1081286513505585

Singh B, 2013. Elastic wave propagation and attenuation in a generalized thermoporoelastic model. *Multidiscipline Modeling in Materials and Structures*, 9(2):256-267. https://doi.org/10.1108/MMMS-04-2013-0032

Tao HB, Liu GB, Xie KH, et al., 2014. Characteristics of wave propagation in the saturated thermoelastic porous medium. *Transport in Porous Media*, 103(1):47-68. https://doi.org/10.1007/s11242-014-0287-6

Wang LJ, Wang LH, 2020. Semianalytical analysis of creep and thermal consolidation behaviors in layered saturated clays. *International Journal of Geomechanics*, 20(4): 06020001. https://doi.org/10.1061/(asce)gm.1943-5622.0001615

Wang N, Wang KH, Wu WB, 2013. Analytical model of vertical vibrations in piles for different tip boundary conditions: parametric study and applications. *Journal of Zhejiang University-SCIENCE A (Applied Physics & Engineering)*, 14(2):79-93. https://doi.org/10.1631/jzus.A1200184

Wen MJ, Xu JM, Xiong HR, 2020. Thermo-hydro-mechanical dynamic response of a cylindrical lined tunnel in a poroelastic medium with fractional thermoelastic theory. *Soil Dynamics and Earthquake Engineering*, 130:105960. https://doi.org/10.1016/j.soildyn.2019.105960

Xue ZN, Yu YJ, Li CL, et al., 2016. Application of fractional order theory of thermoelasticity to a bilayered structure with interfacial conditions. *Journal of Thermal Stresses*, 39(9):1017-1034. https://doi.org/10.1080/01495739.2016.1192451

Xue ZN, Yu YJ, Tian XG, 2017. Transient responses of multi-layered structures with interfacial conditions in the generalized thermoelastic diffusion theory. *International Journal of Mechanical Sciences*, 131-132:63-74. https://doi.org/10.1016/j.ijmecsci.2017.05.054

Xue ZN, Yu YJ, Li XY, et al., 2019. Study of a generalized thermoelastic diffusion bi-layered structures with variable thermal conductivity and mass diffusivity. *Waves in Random and Complex Media*, 29(1):34-53. https://doi.org/10.1080/17455030.2017.1397810

Xue ZN, Tian XG, Liu JL, 2020. Non-classical hygrothermal fracture behavior of a hollow cylinder with a circumferential crack. *Engineering Fracture Mechanics*, 224: 106805. https://doi.org/10.1016/j.engfracmech.2019.106805

Youssef HM, 2007. Theory of generalized porothermoelasticity. *International Journal of Rock Mechanics and Mining Sciences*, 44(2):222-227. https://doi.org/10.1016/j.ijrmms.2006.07.001

Youssef HM, 2010. Theory of fractional order generalized thermoelasticity. *Journal of Heat Transfer*, 132(6): 061301. https://doi.org/10.1115/1.4000705

Yovanovich MM, 2005. Four decades of research on thermal contact, gap, and joint resistance in microelectronics. *IEEE Transactions on Components and Packaging Technologies*, 28(2):182-206. https://doi.org/10.1109/TCAPT.2005.848483

Yuan KL, Wen MJ, Wang WY, et al., 2021. Nonlocal thermodynamic response of thermal insulation layer-substrate wall system considering the temperature-dependent thermal material properties. *Journal of Thermal Stresses*, 44(2):214-235. https://doi.org/10.1080/01495739.2020.1837043

Zhang YP, Liu H, Wu WB, et al., 2021. A 3D analytical model for distributed low strain test and parallel seismic test of pipe piles. *Ocean Engineering*, 225:108828. https://doi.org/10.1016/j.oceaneng.2021.108828

Zhang YP, Jiang GS, Wu WB, et al., 2022. Analytical solution for distributed torsional low strain integrity test for pipe pile. *International Journal for Numerical and Analytical Methods in Geomechanics*, 46(1):47-67. https://doi.org/10.1002/nag.3290

List of electronic supplementary materials

Data S1 Derivation of the analytical solution for Eqs. (25) and (26)

Data S2 Derivation of the analytical solution for medium 2